Models for Bimetallic Catalysts: Anion Additions to Pt_3Re Cluster Cations

Jianliang Xiao, Leijun Hao, and Richard J. Puddephatt*

Department of Chemistry, University of Western Ontario, London, Ontario, Canada N6A 5B7

Ljubica Manojlović-Muir, Kenneth W. Muir,* and Ali Ashgar Torabi

Department of Chemistry, University of Glasgow, Glasgow, Scotland G12 8QQ

Received January 10, 1995[⊗]

The complexes $[Pt_3(\mu_3\text{-}ReL_3)(\mu\text{-}dppm)_3]^+$ (L = CO (**1**), O (**2**)) add halide ions at the Pt_3 face opposite to the ReL_3 fragments to give $[Pt_3(\mu_3\text{-}X)(\mu_3\text{-}ReL_3)(\mu\text{-}dppm)_3]$ (L = CO, X = Cl (**3a**), Br (**3b**), I (**3c**); L = O, X = Cl (**4a**), X = Br (**4b**), X = I (**4c**)). The reactions are easily reversible, with complex stability following the series $X^- = I^- > Br^- > Cl^-$ and L = O > CO. Complex **2** also reacts with SnX_3^- to give $[Pt_3(\mu_3\text{-}SnX_3)(\mu_3\text{-}ReO_3)(\mu\text{-}dppm)_3]$ (X = F, Cl), in which the SnX_3 group caps the Pt_3 triangle. The iodide adduct of **1**, $[Pt_3(\mu_3\text{-}I)\{\mu_3\text{-}Re(CO)_3\}(\mu\text{-}dppm)_3]$ (**3c**), has been characterized by an X-ray crystal structure analysis of **3c**·CH_2Cl_2·H_2O (monoclinic, space group $C2/c$, $a = 34.911(4)$ Å, $b = 19.965(6)$ Å, $c = 24.101(3)$ Å, $\beta = 117.98(1)°$, $Z = 8$, $R = 0.0393$, $R_w = 0.0420$ for 10 848 unique reflections with $I \geq 3\sigma(I)$). The molecular structure of **3c** contains a distorted-tetrahedral Pt_3Re center with the Pt_3 face capped by a weakly bound iodide ligand to form a trigonal-bipyramidal Pt_3ReI core of approximate C_3 symmetry (Pt−Pt = 2.586(1)−2.613(1) Å, Pt−Re = 2.728(1)−2.771(1) Å, and Pt−I = 3.113(1)−3.343(1) Å); the iodide is bound to Pt and not Re as previously proposed.

Introduction

In the Pt−Re−Al_2O_3 catalysts used in petroleum reforming, the platinum is present in the metallic state but rhenium may exist in one or more of the oxidation states Re(0), Re(II), and Re(IV).[1-3] In attempts to model these catalysts, the synthesis and chemistry of several coordinatively unsaturated Pt_3Re clusters have been described.[4] In particular, the oxidation of $[Pt_3\{\mu_3\text{-}Re(CO)_3\}(\mu\text{-}dppm)_3]^+$ (**1**) with O_2 led to the remarkable cluster complex $[Pt_3(\mu_3\text{-}ReO_3)(\mu\text{-}dppm)_3]^+$ (**2**).[4] Since both CO and terminal oxo ligands are 2-electron donors, both complexes **1** and **2** are coordinatively unsaturated 54-electron clusters and they have similar structures, each having a tetrahedral Pt_3Re core.[4] However, while the formal oxidation states of the metals in **1** may be described as $Pt^0{}_3Re^I$, those in **2** can be considered as $Pt^0{}_3Re^{VII}$.[4] The unprecedented existence of two cluster complexes with the same geometry but such widely divergent metal oxidation states gives us an opportunity to study cluster chemistry as a function of the rhenium oxidation state. There is a possibility that such studies may provide clues to how the oxidation state of rhenium in the bimetallic catalysts may influence reactivity. In a preliminary communication, it was shown that neutral ligands such as CO and $P(OR)_3$ add to the rhenium center in **1** but to the Pt_3 center in **2**.[5] The same selectivity was suggested for addition of halide ions on the basis of some spectroscopic properties and by analogy with the neutral ligand additions.[5] However, it has now proved possible to grow crystals of the iodide adduct of **1**, and an X-ray structure determination shows that addition of halide to the Pt_3 center occurs. This paper describes the details of the halide addition reactions to **1** and **2** and also describes some related chemistry of the anions SnX_3^- (X = F, Cl).

With respect to the Pt−Re bimetallic catalysts, it is noted that the alumina-supported re-forming catalysts are chlorinated before use. While one major function of this treatment is to adjust the acidity of the support,[6] it is also thought that chloride also interacts with the metals, influencing the degree of PtRe alloying for example.[7] It is not known how chloride interacts with the metals; perhaps the halide adducts of **1** and **2** may mimic halide coordination of the catalysts.

Results

Synthesis and Spectra of Halide Adducts. Complexes **1** and **2** reacted with halide ions to give the neutral clusters **3** and **4** as shown in eqs 1 and 2.

These reactions are easily reversible, and solutions in CH_2Cl_2 were shown to contain mixtures of starting

[⊗] Abstract published in *Advance ACS Abstracts,* April 15, 1995.

(1) (a) Mingos, D. M. P.; Wales, D. J. *Introduction to Cluster Chemistry*; Prentice-Hall: Englewood Cliffs, NY, 1990. (b) *The Chemistry of Metal Cluster Complexes*; Shriver, D. F., Kaesz, H. D., Adams, R. D., Eds.; VCH: New York, 1990.

(2) Sinfelt, J. H. *Bimetallic Catalysts: Discoveries, Concepts and Applications*, Wiley: New York, 1983.

(3) (a) Fung, A. S.; McDevitt, M. R.; Tooley, P. A.; Kelley, M. J.; Koningsberger, D. C.; Gates, B. C. *J. Catal.* **1993**, *140*, 190. (b) Hilbrig, F.; Michel, C.; Haller, G. L. *J. Phys. Chem.* **1992**, *96*, 9893. (c) Godbey, D. J.; Somorjai, G. A. *Surf. Sci.* **1988**, *202*, 204. (d) Augustine, S. M.; Sachtler, W. M. H. *J. Catal.* **1989**, *116*, 184. (e) Tysoe, W. T.; Zaera, F.; Somorjai, G. A. *Surf. Sci.* **1988**, *200*, 1.

(4) (a) Xiao, J.; Vittal, J. J.; Puddephatt, R. J.; Manojlović-Muir, L.; Muir, K. W. *J. Am. Chem. Soc.* **1993**, *115*, 7882. (b) Xiao, J.; Puddephatt, R. J.; Manojlović-Muir, L.; Muir, K. W.; Torabi, A. A. *J. Am. Chem. Soc.* **1994**, *116*, 1129.

(5) Xiao, J.; Hao, L.; Puddephatt, R. J.; Manojlović-Muir, L.; Muir, K. W. *J. Chem. Soc., Chem. Commun.* **1994**, *2221*.

(6) Gates, B. C. *Catalytic Chemistry*; Wiley: New York, 1992.

(7) (a) Malet, P.; Munuera, G.; Caballero, A. *J. Catal.* **1989**, *115*, 567. (b) Augustine, S. M.; Alameddin, G. N.; Sachtler, W. M. H. *J. Catal.* **1989**, *115*, 217.

0276-7333/95/2314-2194$09.00/0

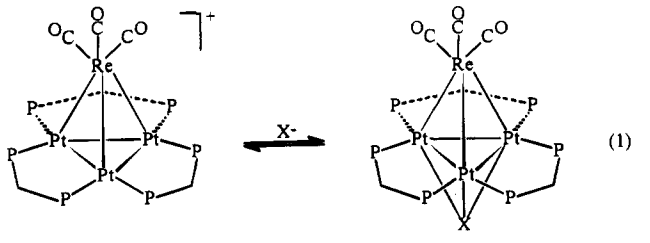

X = Cl, **3a**; Br, **3b**; I, **3c**

(1)

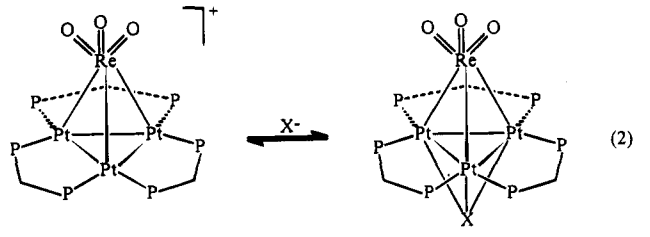

X = Cl, **4a**; Br, **4b**; I, **4c**

(2)

materials and products. However, when the reactions were conducted in acetone solution and in the presence of excess halide, the equilibrium strongly favored product formation and, since the clusters **3** and **4** were sparingly soluble in acetone, they precipitated in high yield. This property makes the isolation of the products easy. The exchange between starting materials and products (eqs 1 and 2) was fast on the NMR time scale, and so only an average signal was observed in either the ^1H or ^{31}P spectra. The NMR parameters of the products **3** and **4** were therefore obtained in CD_2Cl_2 by using excess halide such that the spectroscopic parameters no longer changed with the addition of more halide salt. For each complex **3** or **4**, each ^{31}P NMR spectrum contained only a singlet for the phosphorus atoms of the dppm ligands (an average value for starting materials and products of eq 1 or 2) and the chemical shift moved progressively toward the limiting values quoted for **3** or **4** as more halide was added. Thus, for example, the limiting ^{31}P chemical shifts of **1** and **3b** are δ 7.9 and 4.3, respectively, and in the reaction of **1** with Br^-, the singlet was observed at δ 5.6, 5.2, 4.5, and 4.3 when **1** in CD_2Cl_2 was treated with 1, 1.5, 4, and 10 equiv of bromide, respectively. Qualitatively, when pure **3** or **4** was dissolved in CD_2Cl_2, the equilibrium of eq 1 or 2 lay well to the left when X = Cl, both species were present when X = Br, and the equilibrium lay well to the right when X = I. The halide exchange (eqs 1 and 2) could not be frozen out at temperatures as low as −90 °C. For example, the ^{31}P NMR spectrum of **3b** in CD_2Cl_2 at −90 °C contained a very broad resonance at δ 7.3 with $^1J(PtP)$ = 2472 Hz, tentatively interpreted as being due to an intermediate rate of exchange between **1** and **3b** (Figure 1). The broadening of the spectra at low temperature was initially interpreted in terms of intramolecular fluxionality of an unsymmetrical structure formed by halide addition to the rhenium center,[5] but this is now shown to be incorrect by the X-ray structure determination described below. The broadening at low temperature was much less for **3c**, for which the equilibrium constant is much larger and so which is mostly present as **3** in solution.

The IR spectra of complexes **3** (Nujol mull) contained three bands due to ν(CO) in the terminal carbonyl region. The ν(CO) frequencies were 15−20 cm^{-1} lower in energy than for the parent cluster **1**,[4a] consistent with

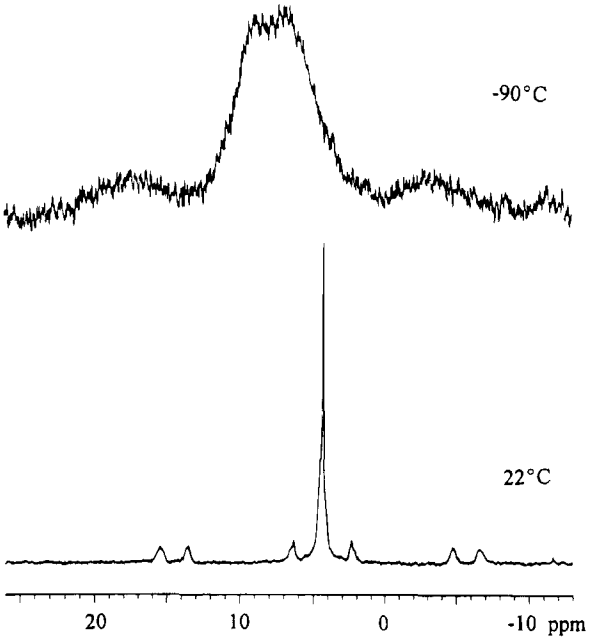

Figure 1. ^{31}P NMR spectra of cluster **3b** in CD_2Cl_2 at 22 °C in the presence of excess bromide to prevent dissociation to **1** and at −90 °C in the absence of excess Br^-. The broadness is interpreted in terms of an intermediate rate of exchange between **1** and **3**. In the room-temperature spectrum, the doublet appearance of the ^{195}Pt satellite spectrum arises from $^3J(PP)$.

slightly stronger Re−CO back-bonding in the neutral clusters **3** compared to the cationic **1**.

The room-temperature ^1H NMR spectra of **3** displayed two resonances of equal intensity for the $CH^aH^bP_2$ protons of the dppm ligands, and the ^{31}P NMR spectra gave singlet resonances at δ 7.0, 4.3, and −5.7 for **3a**−**c**, respectively, with satellites due to coupling to ^{195}Pt, indicative of C_{3v} symmetry on the NMR time scale. The coupling constants $^1J(PtP)$ for **3**, ranging from 2462 to 2520 Hz, are similar to that observed for cluster **1** ($^1J(PtP)$ = 2445 Hz). The ^{195}Pt satellite spectra show a doublet splitting due to the *trans*-like coupling $^3J(PPtPtP)$ through each metal−metal bond (P(1)P(4), P(2)P(5), P(3)P(6) in Figure 2). The long-range couplings $^2J(PtP)$ and $^3J(PP)$, which reflect the strength of Pt−Pt bonding, are similar in magnitude to those found for **1**,[4a] indicating that halide addition does not affect the strength of the Pt−Pt bonds.[8]

The IR spectra of clusters **4** were very similar to that of **2**. For example, the spectrum of **4a** contained bands due to ν(Re=O) at 926 and 890 cm^{-1}, similar to those for cluster **2** (925 and 893 cm^{-1}).[4b] The ReO_3 fragment is also found in [(η^5-C_5Me_5)ReO_3] where the ν(Re=O) bands appear at 909 and 878 cm^{-1}.[9]

The room-temperature ^1H NMR spectra of **4** contained two broad resonances for the $CH^aH^bP_2$ protons and the ^{31}P NMR spectra contained singlets at δ −7.8, −13.9, and −15.2 for **4a**−**c**, respectively, consistent with 3-fold symmetry. The magnitude of the coupling $^1J(PtP)$, ranging between 3210 and 3292 Hz, is slightly larger than that observed for cluster **2** ($^1J(PtP)$ = 3134 Hz).

(8) (a) Rashidi, M.; Puddephatt, R. J. *J. Am. Chem. Soc.* **1986**, *108*, 7111. (b) Ling, S. S. M.; Hadj-Bagheri, N.; Manojlović-Muir, Lj.; Muir, K. W.; Puddephatt, R. J. *Inorg. Chem.* **1987**, *26*, 231.

(9) Herrmann, W. A.; Serrano, R.; Bock, H. *Angew. Chem., Int. Ed. Engl.* **1984**, *23*, 383.

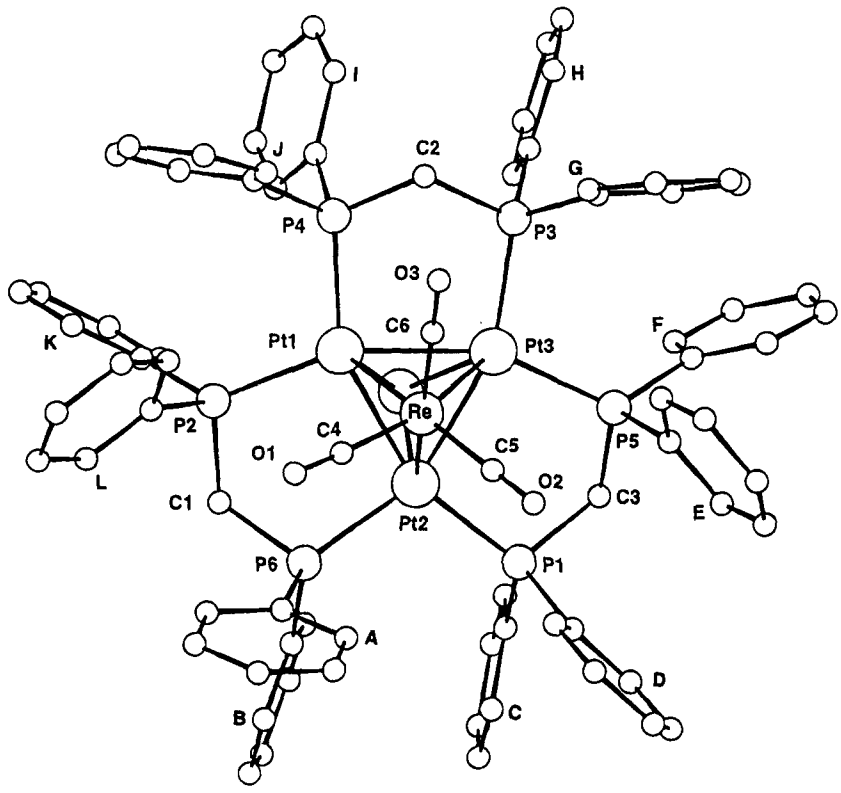

Figure 2. View of the molecular structure of **3c**, with atoms represented by spheres of arbitrary size. In the phenyl rings carbon atoms are numbered in sequences C(n1) to C(n6) (n = A–L) starting with the P-substituted atoms, and the ring labels indicate the positions of the C(n2) atoms. The hydrogen atoms are omitted for clarity.

The values of ^1J(PtP) were significantly higher than in the corresponding complexes **3**.

Structure of Complex 3c. The molecular structure of **3c**, illustrated in Figure 2 and characterized by the atomic parameters listed in Table 1, was determined by an X-ray diffraction study of **3c**·CH_2Cl_2·H_2O. It showed that the addition of halide to the parent complex **1** occurs at the Pt_3 site and not at the Re center as previously thought.[5]

The structure of **3c** contains a triangular Pt_3 unit capped by a $Re(CO)_3$ fragment to form a distorted-tetrahedral Pt_3Re cluster and complete a highly distorted octahedral coordination geometry around the Re center (C–Re–C = 84.1(5)–85.3(5)°, Pt–Re–Pt = 56.0-(1)–57.1(1)°). The other face of the Pt_3 cluster is capped by a weakly bound iodide ligand, resulting in a trigonal-bipyramidal $Pt_3(\mu_3\text{-I})(\mu_3\text{-Re})$ core with approximate C_3 symmetry. The Pt_3 triangle is edge-bridged by three dppm ligands to form a $Pt_3(\mu\text{-dppm})_3$ fragment with an essentially planar Pt_3P_6 skeleton. All three Pt_2P_2C rings adopt envelope conformations with the methylenic carbon atom at the flap and two flaps lying above the $Re(CO)_3$-capped face and the third above the I-capped face of the Pt_3 plane (Figure 3). Such a conformation of the $Pt_3(\mu\text{-dppm})_3$ fragment is characterized by different numbers of axial and equatorial phenyl groups surrounding the opposite faces of the Pt_3 cluster,[10] and the iodide ligand is present on the triangular face associated with lower steric hindrance. It results in approximate C_s symmetry of the $Pt_3(\mu_3\text{-I})\{\mu_3\text{-Re}(CO)_3\}(\mu\text{-P-C-P})_3$ unit, the mirror plane passing through the Pt(2), Re, I, and C(2) atoms and bisecting the Pt(1)–Pt(3) bond. The Pt–P and Re–C bond lengths are unexceptional (Table 2).

In the Pt_3Re core both Pt–Pt (2.586(1), 2.598(1), 2.613(1) Å) and Pt–Re (2.728(1), 2.739(1), 2.771(1) Å) distances display small variations. The mean Pt–Pt (2.60 Å in both **1** and **3c**) and Pt–Re (2.75 Å in **3c** and 2.67 Å in **1**[4a]) distances show that the addition of the iodide donor to the Pt_3 cluster in **3c** has no effect on Pt–Pt bonding but causes lengthening of the Pt–Re bonds. In contrast, addition of the $P(OPh)_3$ donor to the Re site to give the cluster $[Pt_3\{\mu_3\text{-Re}(CO)_3\}\{P(OPh)_3\}(\mu\text{-dppm})_3]^+$ lengthens both Pt–Pt and Pt–Re bonds (mean values 2.64 and 2.84 Å, respectively),[5] and the effect on the Pt–Re bonds is substantially higher than in **3c**.

The Pt–I distances in **3c** (Table 2), which also display small variations, are much longer than the Pt–I bonds (2.806(2)–2.825(2) Å) in $[Pt(\mu_3\text{-I})Me_3]_4$ (where no direct Pt–Pt bonding is observed).[11] It is, however, interesting to compare them with analogous distances in the molecular structures of the closely related complexes $[Pd_3(\mu_3\text{-I})(\mu_3\text{-CO})(\mu\text{-dppm})_3]^+$ and $[Au_3(\mu_3\text{-I})(\mu_3\text{-AuI})(\mu\text{-dppm})_3]$, in which the $Re(CO)_3$ fragment is replaced respectively by CO[12] and AuI[13] units. In all these complexes the M–(μ_3-I) distances are too long to be ascribed to normal covalent bonds. Nevertheless, the Pd–I (2.591(1)–3.083(1) Å), Pt–I (3.113(1)–3.343(1) Å), and Au–(μ_3-I) [3.132(2)–3.668(2) Å] distances follow the order of the metal atom radii Pd < Pt < Au, and both Pd–I and Au–(μ_3-I) distances are considered indicative

(10) Puddephatt, R. J.; Manojlović-Muir, L.; Muir, K. W. *Polyhedron* **1990**, *9*, 2767.

(11) Allman, R.; Kuchazczyk, D. *Z. Kristallogr.* **1983**, *165*, 227.

(12) Lloyd, B. R.; Manojlović-Muir, L.; Muir, K. W.; Puddephatt, R. J. *Organometallics* **1993**, *12*, 1231.

(13) Van der Velden, J. W. A.; Bour, J. J.; Pet, R.; Bosman, W. P.; Noordick, J. H. *Inorg. Chem.* **1983**, *22*, 3112.

of some degree of covalency.[12,13] It would thus appear that there is some covalent character in the Pt–I bonds in **3c**.

Adducts with SnF_3^- and $SnCl_3^-$. The cluster **1** failed to react with SnX_3^- (X = F, Cl), but reaction of **2** with SnX_3^- occurred readily to give **5** as shown in eq 3. The SnX_3^- reagents were generated *in situ* by reaction of SnX_2 with X^-, and with X = F a similar result could also be obtained by making use of $Na[SnF_3]$. No further reaction occurred when excess SnX_3^- was used, in contrast to the similar reaction of $[Pt_3(\mu_3\text{-}CO)(\mu\text{-}dppm)_3]^{2+}$ shown in eq 4.[14–16]

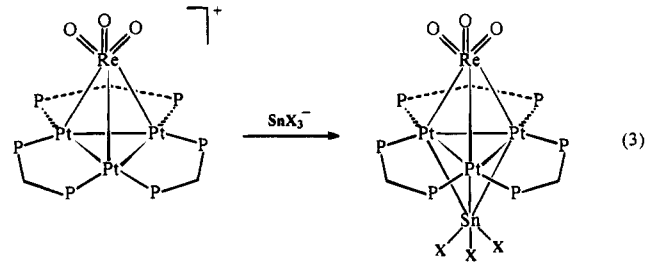

X = Cl, **5a**; F, **5b** (3)

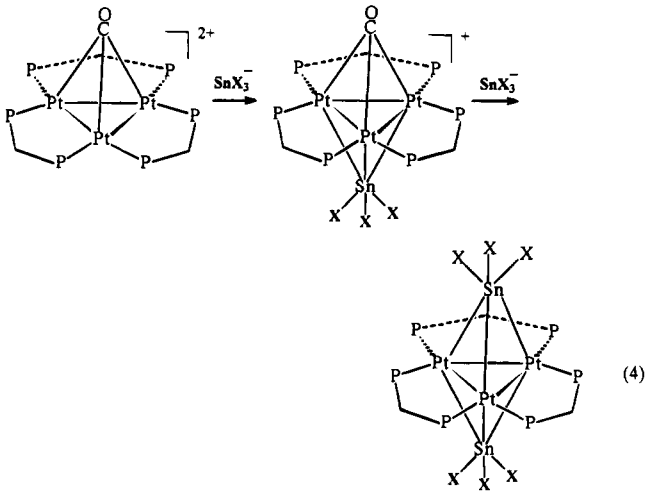

(4)

The IR spectra of **5a** (946 and 937 cm^{-1}) and **5b** (946 and 937 cm^{-1}) each contained two bands assigned to ν(Re=O), the bands occurring at slightly higher energy than in **2** or **4**. The ^{31}P NMR spectra of **5** contained singlet resonances due to the dppm phosphorus atoms, with satellites due to coupling to ^{195}Pt. The couplings $^1J(PtP)$ = 3144 (for **5a**) and 3099 Hz (for **5b**) are close to that for cluster **2** ($^1J(PtP)$ = 3134 Hz).[4] These data support the structure shown in eq 3. In addition, since the NMR spectra in CD_2Cl_2 are independent of added SnX_3^-, it is clear that the equilibrium in eq 3 lies well to the right. It is not clear why **1** fails to form an adduct with SnX_3^-.

Further Studies of the Halide Addition and Exchange Reactions. Consistent with the easy reversibility of the reactions of eqs 1 and 2, anion exchange takes place readily. Thus, in CH_2Cl_2 solution, the chloride ion in **3a** or **4a** was readily replaced by bromide ion to give **3b** or **4b** and the bromide ion in **3b** or **4b** was readily replaced by iodide ion to give **3c** or **4c**, as shown by ^{31}P NMR studies. For example, addition of iodide to a solution of **3b** in CH_2Cl_2, in the presence of excess bromide to prevent dissociation to **1**, led to complete conversion to **3c**. These experiments confirm the ease of the reversibility of the reactions of eqs 1 and 2 and also demonstrate that the equilibrium constants for formation of **3** and **4** follow the sequence $I^- \gg Br^- \gg Cl^-$. This is the sequence expected if the $Pt_3(\mu_3\text{-}X)$ group formed has covalent character in the Pt–X bonding.

It was of interest to determine if **1** or **2** possessed the greater ability to bind halide. This could be studied by using a competition between **1** and **2** for a limited amount of halide. A convenient way to carry out this experiment was to dissolve equimolar amounts of complexes **3b** and **2** in CD_2Cl_2 and to monitor by using ^{31}P NMR. The resulting solution will contain the rapidly equilibrating pairs of compounds **1** (δ 7.9) and **3b** (δ 4.3), and of **2** (δ −2.5) and **4b** (δ −13.9). The ^{31}P NMR spectrum contained two singlets at δ 6.8 for **1** and **3b** and δ −13.8 for **2** and **4b**. Because of the small scale of these reactions, it was difficult to control the stoichiometry accurately and so no attempt was made to obtain the equilibrium constants; nevertheless, it should be clear that bromide is selectively complexed by **2** in competition with **1**. From several experiments, the ratio $K(\mathbf{2})/K(\mathbf{1})$ was estimated to be >10 in competition for the bromide ion.

Discussion

The rhenium centers in complexes **1** and **2** have markedly different oxidation states, but the structures are similar and the cluster electron counts are the same. The neutral ligands CO and $P(OR)_3$ add selectively to the rhenium atom of **1** but to the Pt_3 triangle of **2**.[5] This paper shows that the halide ions add to the Pt_3 triangle of both **1** and **2** while SnX_3^- adds to the Pt_3 triangle of **2** but fails to react with **1**. The cluster **2** therefore shows a consistent pattern of selective reaction at platinum, whereas the cluster **1** may react at either platinum or rhenium, or neither in the case of SnX_3^-. The cluster **2** thus reacts in a way similar to that for the dication $[Pt_3(\mu_3\text{-}CO)(\mu\text{-}dppm)_3]^{2+}$, which adds both neutral and anionic ligands at the Pt_3 triangle opposite to the μ_3-CO group.[10,14] In a comparison of **1** and **2**, the platinum centers in **2** should be more electrophilic, since the ReO_3 group will be more electron withdrawing than the $Re(CO)_3$ group in **1**. This is supported by the observation that the Pt $4f_{7/2}$ binding energy increases from 72.6 to 73.0 eV on going from **1** to **2** and is fully consistent with the observation that **2** binds halide ions more strongly than does **1** and that **2** binds SnX_3^- whereas **1** does not. The coordinative unsaturation in both 54-electron cluster cations **1** and **2** can be considered to be located at a vacant $6p_z$ orbital at each platinum center. If a μ_3-X^- ligand is considered to donate 6 electrons, the clusters **3** and **4** may be considered as coordinatively saturated 60-electron clusters, formed by donation of 2 electrons into each $6p_z$ orbital. The metal–metal bonding in the cluster cation need not be, and indeed appears not to be, perturbed significantly in this process. However, if

(14) Jennings, M. C.; Schoettel, G.; Roy, S.; Puddephatt, R. J.; Douglas, G.; Manojlović-Muir, Lj.; Muir, K. W. *Organometallics* **1991**, *10*, 580.

(15) (a) Lindsey, R. V., Jr.; Parshall, G. W.; Stolberg, U. G. *Inorg. Chem.* **1966**, *5*, 109. (b) Guggenberger, L. J. *J. Chem. Soc., Chem. Commun.* **1968**, 512.

(16) Douglas, G.; Jennings, M. C.; Manojlović-Muir, Lj.; Muir, K. W.; Puddephatt, R. J. *J. Chem. Soc., Chem. Commun.* **1989**, 159.

Table 1. Atomic Fractional Coordinates and Equivalent Isotropic Displacement Parameters (Å²)

	x	y	z	U^a		x	y	z	U^a
Pt(1)	0.13055(1)	0.17229(2)	0.09200(2)	0.027	C(E5)	0.2003(4)	0.4045(3)	0.3928(6)	0.074
Pt(2)	0.09864(1)	0.27702(2)	0.12092(2)	0.027	C(E6)	0.1680(3)	0.3600(6)	0.3564(5)	0.052
Pt(3)	0.14642(1)	0.19153(2)	0.20692(2)	0.027	C(F1)	0.1318(3)	0.1959(3)	0.3462(4)	0.053
Re	0.18542(1)	0.27467(2)	0.15567(2)	0.037	C(F2)	0.1595(4)	0.2056(7)	0.4093(4)	0.071
I	0.04361(2)	0.15004(4)	0.10935(4)	0.054	C(F3)	0.1520(5)	0.1733(7)	0.4539(3)	0.096
P(1)	0.07402(8)	0.33616(12)	0.17986(11)	0.033	C(F4)	0.1167(3)	0.1313(3)	0.4354(3)	0.142
P(2)	0.09668(8)	0.18906(12)	−0.01508(11)	0.031	C(F5)	0.0890(5)	0.1216(7)	0.3724(4)	0.151
P(3)	0.18981(8)	0.10092(12)	0.24955(11)	0.031	C(F6)	0.0965(5)	0.1539(7)	0.3278(3)	0.083
P(4)	0.16879(8)	0.07501(12)	0.11432(11)	0.033	C(G1)	0.2386(4)	0.1177(7)	0.3256(3)	0.039
P(5)	0.13727(8)	0.24237(12)	0.28437(11)	0.035	C(G2)	0.2769(3)	0.1414(3)	0.3292(4)	0.052
P(6)	0.06567(8)	0.32040(12)	0.02274(11)	0.032	C(G3)	0.3100(2)	0.1622(5)	0.3861(4)	0.066
Q(1)	0.2075(3)	0.3406(4)	0.0605(4)	0.074	C(G4)	0.3049(3)	0.1593(6)	0.4394(3)	0.067
Q(2)	0.2309(3)	0.3969(5)	0.2352(5)	0.093	C(G5)	0.2666(3)	0.1356(2)	0.4359(4)	0.076
Q(3)	0.2765(3)	0.2175(5)	0.2077(4)	0.084	C(G6)	0.2335(3)	0.1148(6)	0.3789(4)	0.053
C(1)	0.0551(3)	0.2540(5)	−0.0341(4)	0.037	C(H1)	0.1694(3)	0.0226(3)	0.2656(3)	0.036
C(2)	0.2110(3)	0.0735(5)	0.1960(4)	0.037	C(H2)	0.1978(3)	−0.0273(6)	0.3008(4)	0.049
C(3)	0.0847(3)	0.2863(5)	0.2492(5)	0.042	C(H3)	0.1820(3)	−0.0868(5)	0.3111(5)	0.062
C(4)	0.1977(3)	0.3170(5)	0.0949(5)	0.044	C(H4)	0.1379(3)	−0.0963(3)	0.2862(3)	0.076
C(5)	0.2132(4)	0.3512(6)	0.2056(5)	0.056	C(H5)	0.1095(3)	−0.0463(6)	0.2511(5)	0.074
C(6)	0.2411(4)	0.2400(6)	0.1879(5)	0.056	C(H6)	0.1253(3)	0.0131(5)	0.2407(6)	0.053
C(A1)	0.0970(3)	0.3857(5)	0.0077(3)	0.039	C(I1)	0.1395(4)	−0.0049(5)	0.1028(4)	0.038
C(A2)	0.1193(3)	0.4309(3)	0.0554(4)	0.058	C(I2)	0.1602(3)	−0.0633(7)	0.1322(4)	0.057
C(A3)	0.1455(4)	0.4785(5)	0.0487(4)	0.072	C(I3)	0.1376(3)	−0.1229(5)	0.1180(5)	0.081
C(A4)	0.1494(2)	0.4809(4)	−0.0056(3)	0.081	C(I4)	0.0942(3)	−0.1241(4)	0.0744(3)	0.082
C(A5)	0.1271(3)	0.4356(4)	−0.0533(4)	0.073	C(I5)	0.0735(3)	−0.0657(6)	0.0450(5)	0.069
C(A6)	0.1009(4)	0.3880(6)	−0.0466(4)	0.053	C(I6)	0.0961(3)	−0.0060(4)	0.0592(6)	0.054
C(B1)	0.0102(3)	0.3541(7)	−0.0106(6)	0.038	C(J1)	0.1983(3)	0.0600(3)	0.0688(5)	0.035
C(B2)	−0.0021(3)	0.4136(5)	−0.0435(3)	0.069	C(J2)	0.2398(4)	0.0838(5)	0.0887(3)	0.049
C(B3)	−0.0451(3)	0.4331(4)	−0.0720(5)	0.103	C(J3)	0.2588(3)	0.0787(5)	0.0499(3)	0.059
C(B4)	−0.0757(3)	0.3930(6)	−0.0677(5)	0.083	C(J4)	0.2363(3)	0.0499(3)	−0.0087(4)	0.065
C(B5)	−0.0635(2)	0.3335(4)	−0.0348(3)	0.058	C(J5)	0.1948(3)	0.0261(5)	−0.0286(3)	0.056
C(B6)	−0.0205(3)	0.3140(5)	−0.0062(6)	0.052	C(J6)	0.1758(3)	0.0312(6)	0.0102(4)	0.046
C(C1)	0.0150(3)	0.3528(7)	0.1470(6)	0.043	C(K1)	0.0635(4)	0.1217(5)	−0.0688(3)	0.035
C(C2)	−0.0010(3)	0.4153(5)	0.1228(2)	0.056	C(K2)	0.0741(3)	0.0948(5)	−0.1126(4)	0.054
C(C3)	−0.0449(3)	0.4277(4)	0.0962(5)	0.074	C(K3)	0.0492(3)	0.0439(2)	−0.1516(5)	0.073
C(C4)	−0.0729(2)	0.3775(6)	0.0939(5)	0.070	C(K4)	0.0139(3)	0.0198(4)	−0.1467(3)	0.066
C(C5)	−0.0568(3)	0.3151(4)	0.1181(3)	0.059	C(K5)	0.0033(2)	0.0467(4)	−0.1029(4)	0.061
C(C6)	−0.0129(3)	0.3026(5)	0.1447(6)	0.052	C(K6)	0.0281(4)	0.0976(3)	−0.0640(5)	0.046
C(D1)	0.0980(5)	0.4172(5)	0.2154(5)	0.042	C(L1)	0.1280(3)	0.2167(4)	−0.0538(4)	0.039
C(D2)	0.0814(3)	0.4557(6)	0.2465(4)	0.072	C(L2)	0.1085(3)	0.2458(7)	−0.1126(6)	0.058
C(D3)	0.1012(4)	0.5152(4)	0.2743(6)	0.100	C(L3)	0.1331(3)	0.2631(5)	−0.1415(4)	0.080
C(D4)	0.1377(4)	0.5362(5)	0.2707(4)	0.106	C(L4)	0.1772(3)	0.2512(3)	−0.1116(4)	0.095
C(D5)	0.1543(3)	0.4977(5)	0.2395(5)	0.091	C(L5)	0.1967(3)	0.2221(6)	−0.0528(5)	0.081
C(D6)	0.1345(5)	0.4382(3)	0.2119(7)	0.055	C(L6)	0.1721(3)	0.2049(5)	−0.0239(4)	0.056
C(E1)	0.17775(4)	0.3058(6)	0.3295(3)	0.037	C(7)	0.0575(10)	0.2447(14)	0.6676(13)	0.20(1)
C(E2)	0.2193(4)	0.2961(3)	0.3390(6)	0.050	Cl(1)	0.1130(3)	0.2690(5)	0.6968(5)	0.263(4)
C(E3)	0.2516(3)	0.3406(5)	0.3753(5)	0.065	Cl(2)	0.0359(3)	0.2159(5)	0.7070(5)	0.267(4)
C(E4)	0.2421(3)	0.3948(5)	0.4023(2)	0.068	O(4)	0.5050(7)	0.1112(11)	0.2983(9)	0.25(1)

[a] $U = {}^1/_3\sum_{i=1}^{3}\sum_{j=1}^{3}U_{ij}a^*_i a^*_j(\vec{a}_i\vec{a}_j)$. For the atoms in solvent molecules, C(7), Cl(1), Cl(2), and O(4), U is the isotropic displacement parameter.

a ligand adds to the 18-electron rhenium center of **1** or **2**, it must lead to cleavage or weakening of at least one Pt–Re bond. We suppose that this is only possible if the Re–L bond formed is significantly stronger than the Pt–Re bond broken. This appears to be the case for reaction of **1** with L = CO, $P(OPh)_3$ but not with L = X^-, SnX_3^-. One remaining puzzle is that the binding to **2** follows the sequence $SnX_3^- > I^- > Br^- > Cl^-$ but to **1** the series is $I^- > Br^- > Cl^- > SnX_3^-$.

To gain further insight into the above reactions, an analysis of the interaction of I^- with the model clusters $[Pt_3(\mu_3\text{-}ReL_3)(\mu\text{-}H_2PCH_2PH_2)_3]^+$ (L = CO, O) to give simplified analogues of **3c** and **4c**, $[Pt_3(\mu_3\text{-}I)(\mu_3\text{-}ReL_3)(\mu\text{-}H_2PCH_2PH_2)_3]^+$, has been made using the EHMO method.[17–19] There are bonding interactions between the filled *p* orbitals of I^- and the unoccupied platinum p_z orbitals as shown in **A**. The p_z orbital of I^- interacts

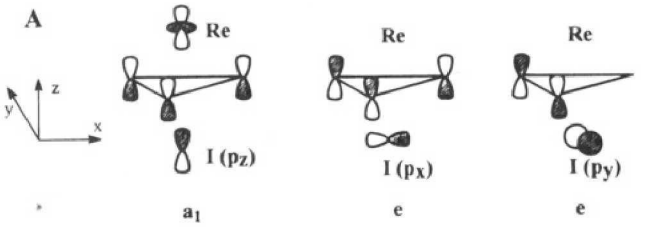

with the a_1 combination of p_z orbitals as shown in **A**, while the p_x and p_y orbitals overlap more weakly with the e combination of p_z orbitals which lie at higher energy. Because of the mismatch in energies of the donor and acceptor orbitals, these bonding interactions are limited and there are also strong interactions involving the filled p orbitals of I^- and filled d orbitals of the Pt_3 unit which cannot lead to a net bonding in either **3c** or **4c**. The a_1 combination of p_z orbitals for cluster **2** is calculated to be more than 1 eV lower in energy than for cluster **1**, and hence a greater bonding interaction is observed for **2**. The calculation for **4c**

(17) For previous theoretical work on Pt_3L_6 clusters, see: (a) Evans, D. G. *J. Organomet. Chem.* **1988**, *352*, 397. (b) Mealli, C. *J. Am. Chem. Soc.* **1985**, *107*, 2245.

(18) Albright, T. A.; Burdett, J. K.; Whangbo, M.-H. *Orbital Interactions in Chemistry*; Wiley: New York, 1985; Chapter 20.

(19) Schoettel, G.; Vittal, J. J.; Puddephatt, R. J. *J. Am. Chem. Soc.* **1990**, *112*, 6400.

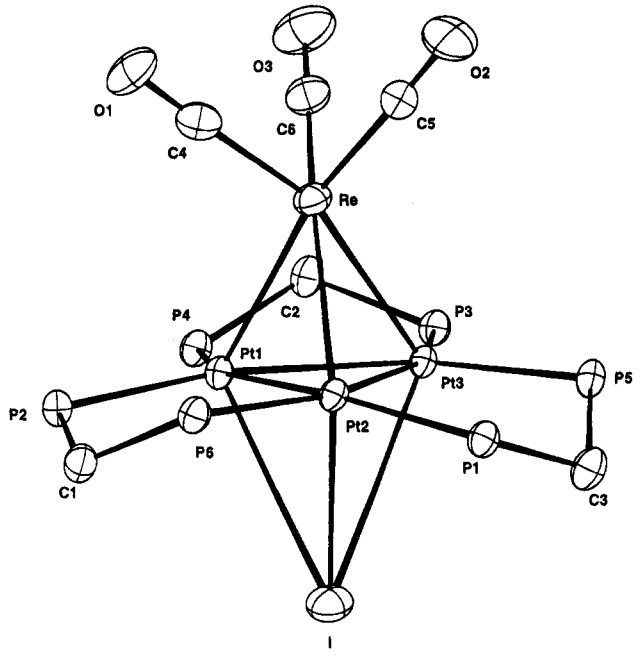

Figure 3. View of the inner core of **3c**, with displacement ellipsoids showing 50% probability.

suggests a charge of only −0.15 e on the coordinated iodide, while the occupation of each $6p_z$ orbital of platinum increased from 0.03 to 0.16 e on addition of iodide. These calculations therefore suggest that, although the net bonding is weak, the $Pt_3(\mu_3\text{-}I)$ interaction is covalent in nature and that iodide can act as a weak six-electron donor by using all of its filled p orbitals in bonding. These results are then in accord with the structural study on **3c** and with the competition experiments between **1** and **2** for halide coordination.

A similar interaction is seen in adding SnF_3^- to the model clusters, but this ligand can act only as a two-electron donor. The donor orbital is the lone pair on tin(II) having mostly tin 5s character.

It may be speculated that halide interacts with the PtRe clusters present in supported bimetallic PtRe catalysts in a way similar to that established here, that is by preferential coordination to platinum.[6,7,20]

Experimental Section

The compounds $[Pt_3\{Re(CO)_3\}(\mu\text{-dppm})_3][PF_6]$ (**1**[PF_6]) and $[Pt_3\{ReO_3\}(\mu\text{-dppm})_3][PF_6]$ (**2**[PF_6]) were prepared by previously reported procedures.[4] IR spectra were recorded by using a Perkin-Elmer 2000 spectrometer, and the NMR spectra were recorded, unless otherwise indicated, in CD_2Cl_2 solution at ambient temperature by using a Varian Gemini-300 spectrometer; chemical shifts are referenced to TMS (^1H) and 85% H_3PO_4($^{31}P\{^1H\}$). Elemental analysis were performed by Guelph Chemical Laboratories and Galbraith Laboratories.

$[Pt_3(\mu_3\text{-Cl})\{Re(CO)_3\}(\mu\text{-dppm})_3]$ (3a). To a solution of **1**[PF_6] (41 mg, 0.019 mmol) in acetone (5 mL) was added tetraethylammonium chloride (3.2 mg, 0.019 mmol). A red-brown precipitate formed almost immediately. The mixture was stirred for 10 min. The solution was then concentrated, followed by adding hexane to completely precipitate the product, which was then washed with acetone (0.5 mL) to give the product as a red-brown powder. Yield: 60%. Anal. Calcd for $C_{78}H_{66}ClO_3P_6Pt_3Re$: C, 45.83; H, 3.25. Found: C, 44.52; H, 4.75. IR (Nujol): ν(CO) 1973 (s), 1862 (s), 1831 (s) cm^{-1}. The NMR spectra of **3a** were obtained by the addition of excess (~10-fold) tetraethylammonium chloride in CD_2Cl_2 solution. Since no detectable change was observed in the NMR spectrum on further addition of the halide, it was assumed that the data given below are the limiting values for **3a**. NMR in CD_2Cl_2: ^1H, δ 6.44 [br, 3H, H^aCP_2], 4.50 [br, 3H, H^bCP_2]; $^{31}P\{^1H\}$, δ 7.0 [s, ^1J(PtP) = 2478 Hz, ^2J(PtP) = 262 Hz, ^3J(PP) = 228 Hz, dppm].

Table 2. Selected Bond Lengths (Å) and Angles (deg)

Pt(1)–Pt(2)	2.613(1)	Pt(1)–Pt(3)	2.586(1)
Pt(1)–Re	2.728(1)	Pt(1)–I	3.283(1)
Pt(1)–P(2)	2.304(3)	Pt(1)–P(4)	2.274(3)
Pt(2)–Pt(3)	2.598(1)	Pt(2)–Re	2.739(1)
Pt(2)–I	3.113(1)	Pt(2)–P(1)	2.301(3)
Pt(2)–P(6)	2.262(3)	Pt(3)–Re	2.777(1)
Pt(3)–I	3.343(1)	Pt(3)–P(3)	2.272(3)
Pt(3)–P(5)	2.275(3)	Re–C(4)	1.905(11)
Re–C(5)	1.905(13)	Re–C(6)	1.857(12)
O(1)–C(4)	1.137(14)	O(2)–C(5)	1.144(16)
O(3)–C(6)	1.185(15)		

Pt(2)–Pt(1)–Pt(3)	60.1(1)	Pt(2)–Pt(1)–Re	61.7(1)
Pt(2)–Pt(1)–I	62.5(1)	Pt(2)–Pt(1)–P(2)	97.1(1)
Pt(2)–Pt(1)–P(4)	153.8(1)	Pt(3)–Pt(1)–Re	62.9(1)
Pt(3)–Pt(1)–I	68.3(1)	Pt(3)–Pt(1)–P(2)	156.6(1)
Pt(3)–Pt(1)–P(4)	93.8(1)	Re–Pt(1)–I	118.5(1)
Re–Pt(1)–P(2)	112.2(1)	Re–Pt(1)–P(4)	109.1(1)
I–Pt(1)–P(2)	98.2(1)	I–Pt(1)–P(4)	109.2(1)
P(2)–Pt(1)–P(4)	109.0(1)	Pt(1)–Pt(2)–Pt(3)	59.5(1)
Pt(1)–Pt(2)–Re	61.2(1)	Pt(1)–Pt(2)–I	69.3(1)
Pt(1)–Pt(2)–P(1)	154.8(1)	Pt(1)–Pt(2)–P(6)	95.7(1)
Pt(3)–Pt(2)–Re	62.7(1)	Pt(3)–Pt(2)–I	71.0(1)
Pt(3)–Pt(2)–P(1)	97.5(1)	Pt(3)–Pt(2)–P(6)	155.1(1)
Re–Pt(2)–I	124.1(1)	Re–Pt(2)–P(1)	120.0(1)
Re–Pt(2)–P(6)	105.9(1)	I–Pt(2)–P(1)	94.6(1)
I–Pt(2)–P(6)	103.2(1)	P(1)–Pt(2)–P(6)	107.2(1)
Pt(1)–Pt(3)–Pt(2)	60.5(1)	Pt(1)–Pt(3)–Re	61.0(1)
Pt(1)–Pt(3)–I	65.8(1)	Pt(1)–Pt(3)–P(3)	97.4(1)
Pt(1)–Pt(3)–P(5)	154.6(1)	Pt(2)–Pt(3)–Re	61.2(1)
Pt(2)–Pt(3)–I	61.791)	Pt(2)–Pt(3)–P(3)	157.9(1)
Pt(2)–Pt(3)–P(5)	94.4(1)	Re–Pt(3)–I	115.1(1)
Re–Pt(3)–P(3)	108.4(1)	Re–Pt(3)–P(5)	112.6(1)
I–Pt(3)–P(3)	112.9(1)	I–Pt(3)–P(5)	99.8(1)
P(3)–Pt(3)–P(5)	107.7(1)	Pt(1)–Re–Pt(2)	57.1(1)
Pt(1)–Re–Pt(3)	56.0(1)	Pt(1)–Re–C(4)	104.6(4)
Pt(1)–Re–C(5)	166.3(4)	Pt(1)–Re–C(6)	106.1(4)
Pt(2)–Re–Pt(3)	56.2(1)	Pt(2)–Re–C(4)	111.9(3)
Pt(2)–Re–C(5)	110.0(4)	Pt(2)–Re–C(6)	157.7(4)
Pt(3)–Re–C(4)	160.2(4)	Pt(3)–Re–C(5)	114.2(4)
Pt(3)–Re–C(6)	103.1(4)	C(4)–Re–C(5)	84.1(5)
C(4)–Re–C(6)	85.3(5)	C(5)–Re–C(6)	84.9(5)
Pt(1)–I–Pt(2)	48.1(1)	Pt(1)–I–Pt(3)	45.9(1)
Pt(2)–I–Pt(3)	47.3(1)	Pt(2)–P(1)–C(3)	108.1(4)
Pt(2)–P(1)–C(C1)	119.3(4)	Pt(2)–P(1)–C(D1)	121.2(5)
C(3)–P(1)–C(C1)	101.3(5)	C(3)–P(1)–C(D1)	101.6(5)
C(C1)–P(1)–C(D1)	102.3(7)	Pt(1)–P(2)–C(1)	108.2(3)
Pt(1)–P(2)–C(K1)	120.1(3)	Pt(1)–P(2)–C(Li)	120.1(4)
C(1)–P(2)–C(K1)	100.2(5)	C(1)–P(2)–C(L1)	104.6(4)
C(Ki)–P(2)–C(Li)	101.0(5)	Pt(3)–P(3)–C(2)	108.7(3)
Pt(3)–P(3)–C(G1)	114.3(5)	Pt(3)–P(3)–C(H1)	122.2(4)
C(2)–P(3)–C(G1)	105.1(5)	C92)–P(3)–C(H1)	122.2(4)
C(G1)–P(3)–C(H1)	102.3(5)	Pt(1)–P(4)–C(2)	110.9(4)
Pt(1)–P(4)–C(I1)	118.7(4)	Pt(1)–P(4)–C(J1)	115.3(3)
C(2)–P(4)–C(I1)	104.9(4)	C(2)–P(4)–C(J1)	104.2(5)
C(I1)–P(4)–C(J1)	101.2(5)	Pt(3)–P(5)–C(3)	109.2(4)
Pt(3)–P(5)–C(E1)	115.7(4)	Pt(3)–P(5)–C(F1)	123.2(3)
C(3)–P(5)–C(E1)	105.5(6)	C(3)–P(5)–C(F1)	98.7(5)
C(E1)–P(5)–C(F1)	102.2(4)	Pt(2)–P(6)–C(1)	109.5(4)
Pt(2)–P(6)–C(A1)	114.8(3)	Pt(2)–P(6)–C(B1)	120.7(5)
C(1)–P(6)–C(A1)	107.3(4)	C(1)–P(6)–C(B1)	97.9(6)
C(A1)–P(6)–C(B1)	104.8(5)	P(2)–C(1)–P(6)	118.1(5)
P(3)–C(2)–P(4)	111.4(6)	P(1)–C(3)–P(5)	114.2(6)
Re(1)–C(4)–O(1)	175.9(9)	Re(1)–C(5)–O(2)	178.0(11)
Re(1)–C(6)–O(3)	179.1(11)		

(20) (a) Godbey, D. J.; Garin, F.; Somorjai, G. A. *J. Catal.* **1989**, *117*, 144. (b) Augustine, S. M.; Sachtler, W. M. H. *J. Catal.* **1987**, *106*, 417. (c) Meitzner, G.; Via, G. H.; Lytle, F. W.; Sinfelt, J. H. *J. Chem. Phys.* **1987**, *87*, 6354.

[$Pt_3(\mu_3$-Br){$Re(CO)_3$}(μ-dppm)$_3$] (3b). A procedure similar to that for **3a** was followed with the use of tetraethylammonium bromide instead of tetraethylammonium chloride. The red-brown solid **3b** was obtained in 76% yield. Anal. Calcd for $C_{78}H_{66}BrO_3P_6Pt_3Re$: C, 44.86; H, 3.19. Found: C, 44.47; H, 3.38. IR (Nujol): ν(CO) 1972 (s), 1861 (s), 1828 (s) cm^{-1}. NMR in CD_2Cl_2: ^{1}H, δ 6.10 [br, 3H, H^aCP_2], 4.41 [br, 3H, H^bCP_2]; $^{31}P\{^1H\}$, δ 4.3 [s, ^1J(PtP) = 2462 Hz, ^2J(PtP) = 259 Hz, ^3J(PP) = 231 Hz, dppm].

[$Pt_3(\mu_3$-I){$Re(CO)_3$}(μ-dppm)$_3$] (3c). Complex **3c** was prepared by the same procedure as for **3a**, except that tetrabutylammonium iodide was used instead of tetraethylammonium chloride. The product was obtained as a dark red-brown powder in 82% yield. Anal. Calcd for $C_{78}H_{66}IO_3P_6Pt_3Re$: C, 43.87; H, 3.12. Found: C, 44.21; H, 3.12. IR (Nujol): ν(CO) 1977 (s), 1866 (s), 1832 (s) cm^{-1}. NMR in CD_2Cl_2: ^{1}H, δ 5.84 [d, 3H, ^2J(HH) = 13.1 Hz, ^2J(PH) = 66 Hz, H^aCP_2], 5.26 [d, 3H, ^2J(HH) = 13.1 Hz, H^bCP_2]; $^{31}P\{^1H\}$, δ = −5.7 [s, ^1J(PtP) = 2520 Hz, ^2J(PtP) = 209 Hz, ^3J(PP) = 240 Hz, dppm]; ^{1}H at −90 °C, δ 5.87 [br, 3H, H^aCP_2], 5.24 [br, 3H, H^bCP_2]; $^{31}P\{^1H\}$ at −90 °C, δ −6.9 [s, br, ^1J(PtP) = 2543 Hz, ^2J(PtP) = 197 Hz, ^3J(PP) = 217 Hz, dppm].

[$Pt_3(\mu_3$-Cl){ReO_3}(μ-dppm)$_3$] (4a). To a solution of **2**[PF_6] (31 mg, 0.015 mmol) in acetone (15 mL) was added tetraethylammonium chloride (9.7 mg, 0.059 mmol). A red-brown precipitate formed almost immediately. The solution was stirred for 15 min and was then concentrated to *ca.* 2 mL. Hexane was added to precipitate the product, which was washed with methanol (0.5 mL) and diethyl ether (2 mL) and then dried under high vacuum to give a red-brown solid. Yield: 70%. Anal. Calcd for $C_{75}H_{66}ClO_3P_6Pt_3Re$: C, 44.86; H, 3.31. Found: C, 44.81; H, 3.37. IR (Nujol): ν(Re=O) of ReO_3 925 (m), 890 (s, br) cm^{-1}. The NMR spectra of **4a** were obtained by the addition of excess tetraethylammonium chloride (15-fold). In the absence of added tetraethylammonium chloride, the NMR spectrum of **4a** in CD_2Cl_2 was very similar to that of **2**, indicating extensive dissociation of chloride under these conditions. NMR for **4a** in CD_2Cl_2: ^{1}H, δ 5.81 [br, 3H, H^aCP_2], 5.30 [br, 3H, H^bCP_2]; $^{31}P\{^1H\}$, δ −7.8 [s, ^1J(PtP) = 3210 Hz, ^3J(PP) = 166 Hz, dppm].

[$Pt_3(\mu_3$-Br){ReO_3}(μ-dppm)$_3$] (4b). The procedure was the same as for **4a**, except that tetraethylammonium bromide was used instead of tetraethylammonium chloride. The red-brown solid **4b** was obtained in 80% yield. In order to characterize **4b** in CD_2Cl_2 solution, a 4-fold excess of tetraethylammonium bromidw was used. Anal. Calcd for $C_{75}H_{66}BrO_3P_6Pt_3Re$: C, 43.89; H, 3.24. Found: C, 43.80; H, 3.42. IR (Nujol): ν(Re=O) of ReO_3 924 (m), 890 (s, br) cm^{-1}. NMR in CD_2Cl_2: ^{1}H, δ 5.80 [br, 3H, H^aCP_2], 5.32 [br, 3H, H^bCP_2]; $^{31}P\{^1H\}$, δ −13.9 [s, ^1J(PtP) = 3292 Hz, ^3J(PP) = 158 Hz, dppm].

[$Pt_3(\mu_3$-I){ReO_3}(μ-dppm)$_3$] (4c). A procedure similar to that for **4b** was followed with the use of **2**[PF_6] and tetrabutylammonium iodide. A red-brown product was obtained. Yield: 90%. **4c** is slightly soluble in dichloromethane. Anal. Calcd for $C_{75}H_{66}IO_3P_6Pt_3Re \cdot {}^1/_2CH_2Cl_2$: C, 42.33; H, 3.15. Found: C, 42.27; H, 2.94. IR (Nujol): ν(Re=O) of ReO_3 926 (m), 892 (s, br) cm^{-1}. NMR in CD_2Cl_2: ^{1}H, δ 5.80 [br, 3H, H^aCP_2], 5.30 [br, 3H, H^bCP_2]; $^{31}P\{^1H\}$, δ −15.2 [s, ^1J(PtP) = 3264 Hz, ^3J(PP) = 174 Hz, dppm]. NMR confirmed the presence of CH_2Cl_2.

[$Pt_3(\mu_3$-$SnCl_3$){ReO_3}(μ-dppm)$_3$] (5a). To a solution of **2**[PF_6] (36 mg, 0.017 mmol) in THF (15 mL) was added an equimolar mixture of NaCl (1.0 mg) and $SnCl_2$ (3.2 mg). After 16 h of stirring, the solvent was removed under vacuum. The brown residue was extracted with dichloromethane to give a brown solution, which was then concentrated to *ca.* 2 mL; the product was precipitated with hexane and then dried under vacuum to give the product in 80% yield. Black platelike crystals of complex **5a** could be obtained from CH_2Cl_2/diethyl ether. Anal. Calcd for $C_{75}H_{66}Cl_3O_3P_6Pt_3ReSn$: C, 40.99; H, 3.03. Found: C, 41.78; H, 3.09. IR (Nujol): ν(Re=O) of ReO_3 946 (m), 937 (s) cm^{-1}. NMR in CD_2Cl_2: ^{1}H, δ 6.05 [br, 3H, H^aCP_2], 5.70 [br, 3H, H^bCP_2]; $^{31}P\{^1H\}$, δ −7.1 [s, ^1J(PtP) = 3144 Hz, ^3J(PP) = 193 Hz, dppm].

[$Pt_3(\mu_3$-SnF_3){ReO_3}(μ-dppm)$_3$] (5b). The same procedure was followed as for **5a** with the use of NaF and SnF_2 instead of NaCl and $SnCl_2$. A yellow-black product was obtained. Yield: 76%. Anal. Calcd for $C_{75}H_{66}F_3O_3P_6Pt_3ReSn$: C, 41.93; H, 3.10. Found: C, 41.67; H, 3.21. IR (Nujol): ν(Re=O) of ReO_3 965 (m), 926 (s) cm^{-1}. NMR in CD_2Cl_2: ^{1}H, δ 5.96 [br, 3H, H^aCP_2], 5.68 [br, 3H, H^bCP_2]; $^{31}P\{^1H\}$, δ −6.6 [s, ^1J(PtP) = 3099 Hz, ^3J(PP) = 122 Hz, dppm].

X-ray Crystal Structure Analysis of [$Pt_3(\mu_3$-I){$Re(CO)_3$}(μ-dppm)$_3$]·CH_2Cl_2·H_2O (3c·CH_2Cl_2·H_2O). A black, needlelike crystal of dimensions ~0.42 × 0.10 × 0.03 mm was used in this analysis. All X-ray crystallographic measurements were made with graphite-monochromated Mo Kα radiation and an Enraf-Nonius CAD4 diffractometer.

The unit cell constants, listed in Table 3, were determined by a least-squares treatment of 25 reflections with Bragg angles 11 < θ < 21°. The intensity data were measured by continuous $\theta/2\theta$ scans of (0.73 + 0.58 tan θ)° in θ, and the scan speeds were adjusted to give $\sigma(I)/I \leq 0.03$ subject to a time limit of 30 s. The stability of the crystal and diffractometer was monitored throughout the experiment by measuring three reflections every 2 h. Their mean intensity showed only random variations not exceeding 3.5%. The integrated intensities of all reflections, derived in the usual manner (q = 0.03),[21] were corrected for Lorentz, polarization, and absorption effects. The last correction was made by the empirical method of Walker and Stuart at the end of the isotropic refinement.[22] The internal agreement factor, R_{int}, for measuring 634 duplicate intensities was 0.034. Of 21 563 unique reflections measured, only 10 848 for which $I \geq 3\sigma(I)$ were used in the structure analysis.

The positions of the Pt and Re atoms were determined from a Patterson function and those of the remaining non-hydrogen atoms from the subsequent Fourier difference syntheses. Hydrogen atoms of the dppm ligands were included in the structural model in calculated positions, with C−H = 0.96 Å and U(H) = 1.2U(C), where U(C) is the isotropic displacement parameter of the carbon atom to which the hydrogen is bonded. No allowance was made for scattering of the hydrogen atoms

Table 3. Crystallographic Data for [$Pt_3(\mu_3$-$Re(CO)_3$)(μ_3-I)(μ-dppm)$_3$]·CH_2Cl_2·H_2O

empirical formula	$C_{79}H_{70}Cl_2IO_4P_6Pt_3Re$
fw	2238.5
space group	C_2/c
a, Å	34.911(4)
b, Å	19.965(6)
c, Å	24.101(3)
β, deg	117.98(1)
V, Å^3	14835(5)
Z	8
D_{calc}, g cm^{-3}	2.004
cryst dimens, mm	0.42 × 0.10 × 0.03
temp, °C	25
radiation	Mo Kα
wavelength, Å	0.71073
μ(Mo Kα), cm^{-1}	80.1
data collection range, θ, deg	2.1−30.0
no. of unique reflns ($I \geq 3\sigma(I)$)	10 848
no. of params refined	701
R	0.0393
R_w	0.0420
largest shift/esd ratio	0.06
observn of unit wt	1.37
final diff synthesis, e Å^{-3}	−1.6 to +1.9

(21) Manojlović-Muir, Lj.; Muir, K. W. *J. Chem. Soc., Dalton Trans.* **1974**, 2427.
(22) Walker, N.; Stuart, D. *Acta Crystallogr.* **1983**, *A39*, 158.
(23) *International Tables for X-ray Crystallography*; Kynoch Press: Birmingham, England, 1974; Vol. IV.
(24) Mallinson, P. R.; Muir, K. W. *J. Appl. Crystallogr.* **1985**, *18*, 51.

of CH_2Cl_2 and H_2O molecules. The structure was refined by full-matrix least-squares, minimizing the function $\sum w(|F_o| - |F_c|)^2$, where $w = \sigma(|F_o|)^{-2}$. The 11 C and H atoms of each phenyl group were refined as a rigid group constrained to D_{6h} symmetry and C−C = 1.38 Å. In the CH_2 groups the hydrogen atoms were allowed to ride on the carbon atoms. All non-hydrogen atoms in the metal complex **3c** were refined with anisotropic, and those in the solvent molecules with isotropic, displacement parameters. The atomic scattering factors and anomalous dispersion corrections were taken from ref 23. The refinement, involving 701 parameters and 10 848 unique reflections with $I \geq 3\sigma(I)$, converged at $R = 0.0393$ and $R_w = 0.0420$.

All calculations were performed using the GX program package.[24]

Acknowledgment. We thank the NSERC (Canada) for financial support and the SERC (U.K.) for an equipment grant and the Iranian government for a studentship (to A.A.T.).

Supplementary Material Available: Tables of hydrogen atom coordinates, anisotropic displacement parameters, and bond lengths and angles for **3c** (7 pages). Ordering information is given on any current masthead page.

OM950016B